Probabilistic Estimates of Tsunami Risk for Small Craft Marinas

Adam S. Keen, S.M.ASCE[1]; Patrick J. Lynett, M.ASCE[2]; Martin L. Eskijian, M.ASCE[3]; Aykut Ayca[4]; and Rick I. Wilson, A.M.ASCE[5]

Abstract: Since the 2006 Kuril Islands tsunami, California small craft marinas have sustained over $100 million in total damage from tsunami events. Surveys conducted after the 2006 Kuril Islands and 2011 Japan tsunamis indicated that the mooring systems (e.g., cleats and pile guides) responsible for keeping the vessels and floating docks in place during an event are susceptible to failure. The aim of this paper is to present a risk framework that can be used by decision makers to assess future tsunami risks to small craft marinas. Here, the coupling of high-resolution numerical modeling and an existing statistical framework is extended to include observed damage states for structural elements. When applied to one small craft marina (in Noyo River Harbor), our methodology was able to replicate likely failure, which occurred well below previously identified damage thresholds. The results suggest infrastructure age and condition, in addition to the hazardous tsunami phenomenon, can contribute to cleat and pile guide failure. **DOI: 10.1061/(ASCE)WW.1943-5460.0000599**. © *2020 American Society of Civil Engineers*.

Introduction

The California coastline, and especially the infrastructure in its ports and harbors, is susceptible to damaging tsunamis from both local and distant tsunami sources. During the tsunamis of 2006 from the Kuril Islands, 2010 from Chile, and 2011 from Japan, California harbors sustained over $100 million in total damage (Wilson et al. 2013). Harbors including Crescent City Harbor, Noyo River Harbor, and Santa Cruz Harbor were among those that saw the greatest impact from the 2011 Japan tsunami (Wilson et al. 2013). The damage survey conducted after the events showed that the mooring systems responsible for keeping the vessels and floating docks in place commonly fail (Dengler et al. 2009; Wilson et al. 2013).

Structural failures of this type and magnitude suggest harbor improvements and mitigation measures could greatly reduce tsunami damage from future events. A study headed by the U.S. Geological Survey (USGS) indicated that although a large, distant-source tsunami (i.e., from Alaska) could cause tens of billions of dollars of damage to coastal ports and harbors, 80%–90% of that damage could be reduced by implementing tsunami mitigation and related resilience strategies (Ross et al. 2013). These resilience strategies could not only reduce the direct damage to the harbors but also significantly improve recovery times.

With limited resources available across all levels of government, optimizing the return on investment is the primary consideration for decision makers. Project value for any mitigation or resilience strategy is related to increased levels of safety for small craft harbors. To better assist harbors with pre-tsunami mitigation, local, state and federal entities generally require a predictive tool to understand the future risk to small craft harbors.

Risk, in a very basic sense, can be defined as the product of hazard and vulnerability. The term hazard relates to the probability of occurrence of a potentially damaging phenomenon (Dewan 2013). Vulnerability relates to the degree of loss that results from the occurrence of the phenomenon (Dewan 2013). Developing and applying a consistent risk framework by equitably characterizing the tsunami hazard and harbor vulnerability across multiple harbors is the key to helping decision makers understand the value of mitigation and resilience strategies.

For tsunamis in small craft harbors, "potentially damaging phenomenon" include significant changes in water surface elevation as well as associated strong currents. Handling the tsunami hazard in small craft harbors in a probabilistic framework remains an area of active research and studies are limited. Instead, authors typically opt for a deterministic approach, assessing several historic events or likely scenarios to quantify the hazard. Globally, several authors (Borrero and Goring 2015; Borrero et al. 2015a, b; Lynett et al. 2012) have assessed the tsunami hazard. Barberopoulou et al. (2011), Lynett et al. (2014) and Keen et al. (2017) specifically addressed tsunami hazards within California ports, harbors, and marinas.

Existing methodologies to characterize harbor vulnerability and predict damage to small craft harbors during tsunami events are limited. Approaches vary but the methodologies that do exist have largely been data-driven, relying on correlations between input parameters and documented damage. For instance, using damage reports from the 2011 Tōhoku tsunami in Japan, Suppasri et al. (2014) derived independent loss functions for maximum tsunami surface elevation and maximum flow velocities using linear regression analysis assuming a logarithmic loss function. Muhari et al. (2015) extended the work of Suppasri et al. (2014) to develop new multivariate loss functions to estimate the potential damage of

[1]Graduate Student, Sonny Astani Dept. of Civil and Environmental Engineering, Univ. of Southern California, Los Angeles, CA 90089 (corresponding author). ORCID: https://orcid.org/0000-0002-8236-0848. Email: adamkeen@usc.edu

[2]Professor, Sonny Astani Dept. of Civil and Environmental Engineering, Univ. of Southern California, Los Angeles, CA 90089. Email: plynett@usc.edu

[3]Senior Engineer, California State Lands Commission, Long Beach, CA 90802. Email: mleskijian@gmail.com

[4]Present Address: Scientist 1, AIR Worldwide, Boston, MA 02116; Previously: Graduate Student, Sonny Astani Dept. of Civil and Environmental Engineering, Univ. of Southern California, Los Angeles, CA 90089. Email: aayca@air-worldwide.com

[5]Senior Engineering Geologist, California Geological Survey, Sacramento, CA 95814. Email: rick.wilson@conservation.ca.gov

Note. This manuscript was submitted on November 26, 2019; approved on April 23, 2020; published online on September 24, 2020. Discussion period open until February 24, 2021; separate discussions must be submitted for individual papers. This paper is part of the ***Journal of Waterway, Port, Coastal, and Ocean Engineering***, © ASCE, ISSN 0733-950X.

marine vessels. Lynett et al. (2014) compared damage reports for five California small craft marinas with numerically modeled current speeds within each harbor. The semi-quantitative approach was able to correlate the current speed thresholds with basic thresholds of damage. Keen et al. (2017) developed a Monte Carlo physics-based approach to estimate damage levels to cleats and pile guides. The authors' method, however, did not consider infrastructure deterioration with time, which should result in a decrease in strength or capacity and increased probability of failure.

The aim of this paper is to present a risk framework that can be used by decision makers to assess existing and future tsunami risks to small craft harbors in California. Coupling of high-resolution numerical modeling with the statistical framework outlined by Keen et al. (2017) is extended to include observed damage states for structural elements in small craft harbors to quantitatively estimate risk. Section "Cleat and Pile Guide Demand" will briefly outline the statistical fragility curve methodology presented by Keen et al. (2017). Section "Cleat and Pile Guide Capacities" will summarize results from the small craft harbor inspection program. The program, which included 12 California small craft harbors, focused on empirically estimating installed capacities as well as damage states of structural elements in harbors. The risk methodology will be outlined in the section titled "Damage Prediction for Small Craft Harbors" and applied to Noyo River Basin in Northern California in "Case Study: Noyo Harbor" section. Conclusions are summarized in "Conclusions."

Cleat and Pile Guide Demand

Cleat and pile guide tsunami demand in small craft harbors is estimated using fragility curves. Only an abridged statistical methodology to estimate tsunami demand is summarized here for completeness. For a full description of the methodology, the reader is referred to Keen et al. (2017).

Fragility curves for structural components in small craft harbors are estimated using a Monte Carlo methodology. For background, a Monte Carlo-based approach in structural analysis is a probabilistic tool in which the governing equations of motion or structural behavior might be well known but the independent variables of the input (i.e., current speed, current direction) as well as the structural capacities of the components (e.g., cleats, pile guides) might not be. The Monte Carlo approach requires a distribution of each input variable (usually with a rectangular-, triangular-, or Gaussian-shaped relationship), and then randomly samples each distribution within the described equations to generate a single computational result. The process repeats hundreds or thousands of times, depending on the required accuracy and convergence of the system.

Cleats

The governing equations for the transverse and longitudinal forces on vessels were used to calculate the "demand" from the tsunami current (USACE, NAVFAC, AFCESA 2005). The equations to determine the current forces on the vessels are summarized in this section. The approach is intended to be first order in identifying the initiation of damage; differential loads and debris loadings are not treated in this phase of the analysis.

For the transverse current forces on a vessel (USACE, NAVFAC, AFCESA 2005), we have

$$F_{yc} = \frac{1}{2}\rho_w V_c^2 L_{wl} T\, C_{yc} \sin\theta \tag{1}$$

where ρ_w = water density; V_c = current velocity; L_{wl} = length of the vessel at the waterline; T = vessel draft; C_{yc} = transverse drag coefficient; and θ = angle of velocity relative to the vessel longitudinal axis. The transverse drag coefficient (USACE, NAVFAC, AFCESA 2005) is dependent upon the vessel dimensions and water depth (Keen et al. 2017).

Similarly, the expression for the longitudinal current forces on the vessel, not considering propeller loads, which could be highly variable (USACE, NAVFAC, AFCESA 2005), is

$$F_{xc} = F_{x\,\mathrm{FORM}} + F_{x\,\mathrm{FRICTION}} \tag{2}$$

with

$$F_{x\,\mathrm{FORM}} = \frac{1}{2}\rho_w V_c^2 B\, T\, C_{xcb} \cos\theta \tag{3}$$

where C_{xcb} = longitudinal current form drag coefficient (= 0.1), and

$$F_{x\,\mathrm{FRICTION}} = \frac{1}{2}\rho_w V_c^2 B\, S\, C_{xca} \cos\theta \tag{4}$$

where S = wetted surface area; and C_{xca} = longitudinal current skin friction coefficient. The longitudinal current skin friction coefficient is a function of the Reynolds number, defined for vessels in terms of the current velocity, current direction and vessel length (Keen et al. 2017). The wetted surface area is defined as (USACE, NAVFAC, AFCESA 2005)

$$S = 1.7\, T\, L_{wl}^2 + \left(\frac{D}{T\,\gamma_w}\right) \tag{5}$$

where γ_w = weight density of water; and D = vessel displacement.

The total tsunami demand can be defined as the magnitude of the directional components

$$\mathrm{Demand} = \sqrt{F_{xc}^2 + F_{yc}^2} \tag{6}$$

Vessels resist the tsunami demand via their cleat connection. The analysis presented here assumes that these cleats act as a system distributing the load evenly across the cleats. Small craft harbors within California generally secure each vessel within the slip using either a 2- or 4-cleat configuration. These types of cleats are usually mounted on the dock with two bolts via a timber connection. By knowing the size and number of bolts, the capacities for each cleat can be directly estimated (to be discussed more in the section titled "Cleat and Pile Guide Capacities").

Pile Guides

To estimate the pile guide demand, Keen et al. (2017) apply the same equations used to estimate the longitudinal and transverse forces on the vessels to the floating dock infrastructure. The equations used to describe the hydrodynamic loads from the tsunami on the floating dock system are the same equations applied to estimate the vessel demand except (for floating docks) the structural demand is 90° out of phase with the vessel orientation (perpendicular to the fingers/vessels); the fingers are in the same line as the vessels (Keen et al. 2017).

Floating docks and fingers resist the hydrodynamic tsunami demand via the pile guide (Keen et al. 2017). Forces on the pile guides are determined based upon the demand equations. Keen et al. (2017) then show the floating dock demand can be averaged based upon the number of pile guides to determine the average load per pile guide. Multiple pile guides within a dock system resist horizontal loads while allowing the dock to adjust to a rising and falling tide. For the pile guide capacity in California marinas, a typical pile guide collar will consist of between four and eight bolts that connect to the dock via a timber connection.

Cleat and Pile Guide Capacities

Within a demand/capacity framework, the capacity of the system plays a key role in determining the probability of failure. As a tsunami enters a harbor, the tsunami currents will generate a demand on the system. No matter how weak these currents are, there must be enough capacity to resist the demand from the tsunami currents. Engineers typically think of structural loads in terms of a design capacity. However, over time, aging infrastructure will result in decreased structural capacity (or increased vulnerability). A harbor that may have once resisted a tsunami current with new cleats and pile guides has the potential to experience a significant decrease in the structural capacity and the inherent increase in risk, without sufficient upkeep.

To better understand how aging structural components, increase a harbor's vulnerability to tsunami currents, an extensive field survey was conducted of small craft harbors within California. Twelve harbors within California were surveyed and are shown in Fig. 1. Harbor locations ranged from the northernmost harbor in California, Crescent City, to Oceanside Harbor in San Diego County along the US southern border. Harbors were selected based upon known vulnerability to tsunami events [Wilson et al. (2013) provide an exhaustive listing of known tsunami damage from the 2010 Chile and 2011 Tōhoku tsunamis] and the degree of cooperation from the local owners. Considerations also included selection to cover the full range of harbor configurations, climatic conditions, and infrastructure age.

The framework for the surveys was developed based upon the methodologies outlined in *Waterfront Facilities Inspection and Assessment* (Waterfront Inspection Task Committee 2015). The surveys focused on two critical components: the cleats and pile guides. At each harbor the survey team would evaluate each dock segment and photograph a representative sample of cleats and pile guides. Care was taken to ensure the sample was sufficiently large to cover the full parameter space as well as randomized to minizine observational bias. Surveys could last up to 5 h but depended on the size of the harbor, condition of the docks, and degree to which the harbor allowed access.

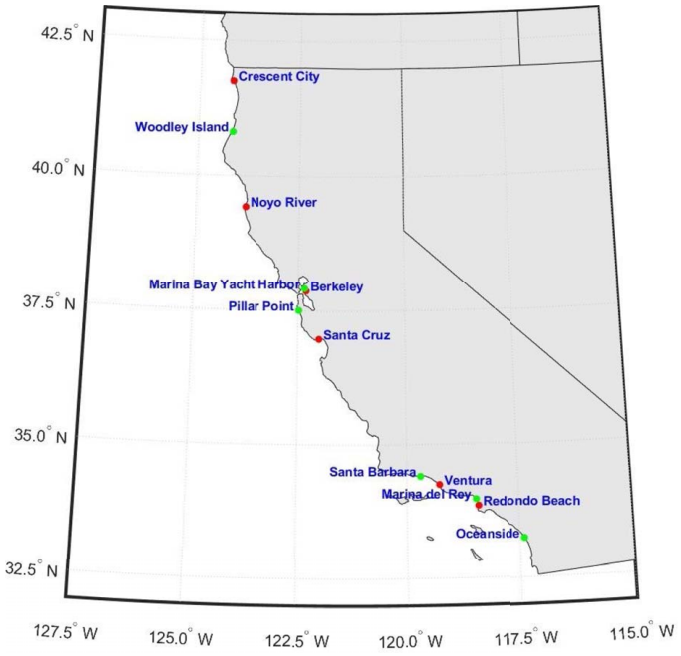

Fig. 1. California small craft harbors surveyed.

The field campaign identified one type of cleat and three types of pile guides: the hoop-type, the roller-type, and the high-density polyethylene (HDPE) pile guide. The framework outlined by the Waterfront Inspection Task Committee (2015) depends on first estimating the capacity of a newly and properly installed element (listed as "No Defects"). Damage states (ranging from "Minor" to "Severe") are then assigned to observable defects in each element. To incorporate the damage states into the probabilistic damage model, reduction factors (ranging from 1.0 for the "No Defects" state to 0.25 for the "Severe" state) are applied to the capacity of each element based upon the damage state.

The survey of California harbors and the photo analysis indicated that cleat and pile guide conditions within a harbor largely center around an expected mean with some natural variably. Expert judgment was used to construct a trapezoidal distribution (Fig. 2) for each damage state that allows natural variability in each damage state to be included in the probabilistic model. The five damage class distributions (from Fig. 2) are: no damage (ND), minor damage (MN), moderate damage (MD), major damage (MJ), and severe damage (SD) [consistent with the damage states outlined by Waterfront Inspection Task Committee (2015) and those published in this paper].

Cleats

Site visits to the 12 harbors identified only one type of cleat used to connect vessels to floating docks. A sample of this style of cleat is shown in Fig. 3. Cleat sizes ranged from 8 in. for smaller vessels to 24 in. for the largest vessels. The cleat is connected to the dock through the whaler with two bolts. A survey of marine cleat manufacturers indicated that increasing cleat size corresponds to an increased bolt size. The survey also suggests that the cleat/bolt pairs have been standardized by the maritime industry. The equation to determine cleat capacity is

$$\text{Capacity}_{\text{Cleat}} = \alpha\,\gamma\,n_{\text{bolt}}\sigma_{\text{bolt}} \tag{7}$$

where α = capacity reduction factor; γ = capacity calibration factor (O[2]); n_{bolt} = number of bolts (generally two); and σ_{bolt} = bolt tension capacity. The form of this equation is consistent with the expected cleat failure mode (pullout or tension failure) with the added term α representative of the cleat's aging, weathering, and decreased capacity.

Observed damage states and empirical capacity reduction factors for cleats are provided in Table 1. The damage states closely relate the amount of corrosion and pitting to the remaining capacity of the cleat. One important note is that the amount of pitting/corrosion on the cleat does not directly relate to damage of the cleat itself. Typically, it is the bolts that fail and pull the cleat out of the dock. Observations from the field indicate the amount of cleat pitting/corrosion is a reasonable indicator of the remaining cleat capacity (Waterfront Inspection Task Committee 2015). In cases in which cleats fail, dock managers normally opt to replace both the cleat and bolts instead of replacing only the bolts and leaving the corroded cleat.

Hoop-Type Pile Guides

The hoop-type pile guide is one of three types identified during the field survey, commonly used in harbors that support their floating docks with round piles. A sample of this style of hoop-type pile guide is shown in Fig. 4. This type of pile guide consists of a section of metal pipe curved into a C-shape that wraps around the pile. The hoop is then connected to the dock by a metal bracket bolted through the whalers with either two or four bolts. The two metal segments are either welded or bolted together. Like the cleats,

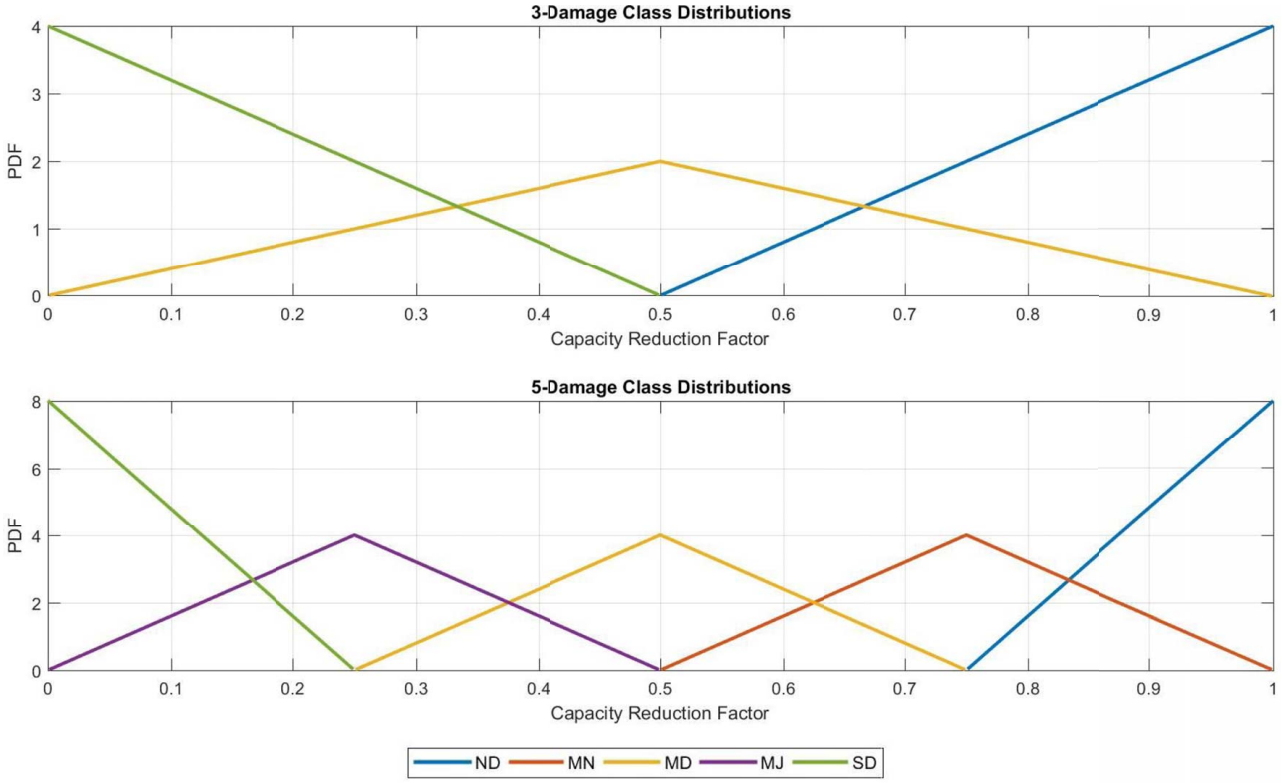

Fig. 2. Capacity reduction factor distributions determined based upon observable degradation. The five damage class distributions are: no damage (ND), minor damage (MN), moderate damage (MD), major damage (MJ) and severe damage (SD) [consistent with the damage states outlined by Waterfront Inspection Task Committee (2015)].

Fig. 3. Typical cleat configuration for California small craft harbors. (Reprinted from Keen et al. 2017, ©ASCE.)

failure modes for this system indicate that heavy corrosion and/or bolt pullout failure are the most common failure modes.

The equation to determine the hoop-type pile guide capacity is

$$\text{Capacity}_{pg-\text{hoop}} = \alpha\gamma n_{\text{bolt}}\sigma_{\text{bolt}} \quad (8)$$

Observed damage states for hoop-type pile guides are given in Table 2. The form of this equation is consistent with the expected hoop-type failure mode (shear failure) with the added term α representative of the pile guide's aging and decreased capacity with increased design life.

The damage states closely relate the amount of corrosion and pitting to the remaining capacity of the pile guide. In cases where extreme corrosion resulting in section loss has occurred, the above equation does not actually capture the failure mode. However, with failure capacities at 20% of the remaining design capacity, this approximation should be representative of the reduced capacity mode.

Roller-Type Pile Guides

The roller-type pile guide, used in harbors that support their floating docks with square piles, is the second of the three types of pile guides identified during the field survey. A sample of this type of pile guide is shown in Fig. 5. Roller-type pile guides consist of a mounting bracket bolted to the floating dock. The pile roller is frequently bolted to this bracket using two bolts. Unlike cleats and hoop-type pile guides, which are largely maintenance free, the roller that defines the roller-type pile guide requires frequent maintenance. The roller must be able to slide along the pile and adjust to changes in water level. If the roller cannot move freely, the dock will become pinned up against the pile and likely fail. This added step requires facilities managers to regularly assess all rollers at their facility and replace the assembly should it not have proper movement. Unlike the cleat and hoop-type pile guide, which experience "pullout failure," roller-type pile guides can experience shear failure during a tsunami event. The equation to determine

Table 1. Damage ratings and capacity reduction factors for cleats

Class	Damage rating		Existing damage	Capacity reduction factor
—	NI	Not inspected	• Not inspected, inaccessible, or passed by	—
1	ND	No damage	• Cleat material sound; surfaces are smooth without indication of corrosion • No surface wear or evidence of pitting	1.0
2	MN	Minor damage	• Cleat has corrosion over 10% to 25% of surface area • Minor surface wear or pitting on surface of cleat	0.75
3	MD	Moderate damage	• Cleat has corrosion over 25% to 50% of surface area • Moderate surface wear or pitting of cleat	0.50
4	MJ	Major damage	• Cleat has corrosion over 50% to 75% of surface area • Significant surface wear or pitting of cleats	0.25
5	SD	Severe damage	• Cleat has corrosion over more than 75% of surface area • Structural displacement, deformation, or rotation of cleat • Loose, broken, or missing fasteners	0.0

Note: —, not applicable.

Fig. 4. Typical hoop-type pile guide configuration for California small craft harbors. (Reprinted from Keen et al. 2017, ©ASCE.)

the roller-type pile guide capacity is defined as

$$\text{Capacity}_{pg-\text{roller}} = \alpha\,\gamma\,n_{\text{bolt}}\,\tau_{\text{bolt}} \tag{9}$$

where τ_{bolt} = bolt shear capacity. The form of this equation is consistent with the expected failure mode (shear failure) with the added term α representative of the pile guide's aging and decreased capacity with increased design life.

Observed damage states for hoop-type pile guides are presented Table 3. Much like cleat and hoop-type pile guide failure, the damage states for roller-type pile guides closely relate the amount of corrosion and pitting to the remaining capacity of the pile guide. However, for roller-type pile guides, we only defined three typical damage states

Table 2. Damage ratings and capacity reduction factors for hoop-type pile guides

Class	Damage rating		Existing damage	Capacity reduction factor
—	NI	Not inspected	• Not inspected, inaccessible, or passed by	—
1	ND	No damage	• Pile guide material sound; surfaces are smooth without indication of corrosion • No surface wear or evidence of pitting	1.0
2	MN	Minor damage	• Pile guide shows evidence of moderate corrosion • Moderate surface wear or pitting of pile guide	0.75
3	MD	Moderate damage	• Pile guide shows evidence of major corrosion with no section loss	0.50
4	MJ	Major damage	• Pile guide shows evidence of major corrosion with fractional section loss • Major surface wear or pitting of pile guide	0.25
5	SD	Severe damage	• Pile guide shows evidence of major corrosion with missing section • Structural displacement, deformation, or rotation of pile guide • Loose, broken, or missing fasteners	0.0

Note: —, not applicable.

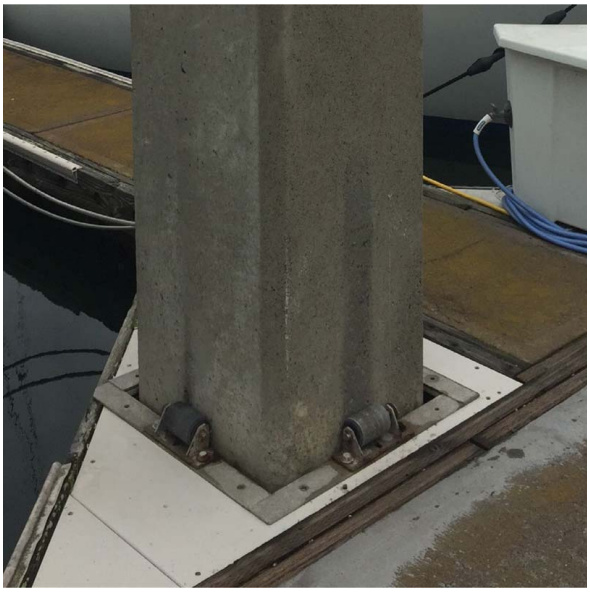

Fig. 5. Typical roller-type pile guide configuration for California small craft harbors. (Image by Adam S. Keen.)

(instead of five). Photos from the field visits suggest that refining the damage states into more groups was difficult given the first order magnitude and purpose of this methodology. Adjusting the probability density functions that define uncertainty in the capacity reduction factors should capture the uncertainty in the damage states.

High-Density Polyethylene (HDPE) Pile Guides

The final type of pile guide typical of small craft harbors in California is the high-density polyethylene (HDPE) pile guide. An example of

Table 3. Damage ratings and capacity reduction factors for roller-type pile guides

Class	Damage rating		Existing damage	Capacity reduction factor
—	NI	Not inspected	• Not inspected, inaccessible, or passed by	—
1	ND	No damage	• Pile guide material sound; surfaces are smooth without indication of corrosion • No surface wear or evidence of pitting	1.0
2	MD	Moderate damage	• Pile guide has corrosion over 25% to 50% of surface area • Moderate surface wear or pitting of pile guide	0.50
3	SD	Severe damage	• Pile guide has corrosion over more than 75% of surface area • Structural displacement, deformation, or rotation of pile guide • Loose, broken, or missing fasteners	0.0

Note: —, not applicable.

Fig. 6. Typical high-density polyethylene (HDPE) pile guide configuration for California small craft harbors. (Image by Adam S. Keen.)

an HDPE pile guide is shown in Fig. 6. This type of pile guide represents a technology advancement, and is ordinarily found in newly built harbors or harbors that experienced damage from the 2010 Chile or the 2011 Tōhoku tsunamis. For instance, Crescent City Harbor, which was nearly destroyed in the 2011 Tōhoku tsunami, replaced all the pile guides in the harbor with HDPE pile guides.

One advantage of HDPE pile guides is that they are nearly maintenance free. The pile guides are not vulnerable to corrosion like hoop-type pile guides, nor do they require regular servicing like a roller-type pile guide. However, since HDPE pile guides represent newly built construction, developing an understanding of the failure modes and aging process is not currently possible. Therefore, we used the model of the roller-type pile guide, assuming that the reduction in the coefficient of static friction between concrete/steel and concrete/HDPE reasonably captures the capacity of a newly built HDPE pile guide.

The equation to determine the capacity of a HDPE pile guide is defined as

$$\text{Capacity}_{pg-\text{HDPE}} = 2.5\ (2\gamma\ \tau_{\text{bolt}}) \tag{10}$$

where 2.5 represents the ratio between the static friction between steel and HDPE (Zhang 2016) and steel and concrete (Rabbat and Russell 1985); and 2 is representative of the number of bolts of an equivalent roller-type pile guide. To reiterate, as the HDPE pile guide is a relatively new construction, an age reduction factor is not included in Eq. (10).

Damage Prediction for Small Craft Harbors

The intent of this demand/capacity framework is to provide harbor maintenance and decision makers with a tool to better understand future risk to small craft harbors. In this section, the probabilistic damage (risk) methodology is outlined for California marinas. The methodology is applied to a small craft harbor in Northern California, Noyo River Harbor, in "Case Study: Noyo Harbor."

Numerical Modeling

The first decision that planners need to make when applying the demand/capacity methodology is whether to estimate the tsunami hazard in a probabilistic or deterministic sense. For the first iteration of the model, we chose to apply the methodology deterministically due to the lack of offshore tsunami hazard curves and because of the high computational cost required to estimate current speed hazard curves at parcel scales within the harbor.

We applied the hydrodynamic model Method of Splitting Tsunamis (MOST) (Titov and Gonzalez 1997; Titov and Synolakis 1998) to 12 small craft marinas in California. MOST simulates the principle phases of tsunami propagation from initial generation, through propagation, and wave run-up (including wave breaking). Initial wave generation in MOST is modeled with elastic deformation theory from Okada (1985). Wave propagation and inundation are modeled based upon a derivation of the model published by Titov and Synolakis (1998). MOST variants have been in constant use for tsunami hazard assessments in California since the mid-1990s (e.g., Lynett et al. 2014). MOST has also been validated as part of the National Tsunami Hazard Mitigation Program model benchmarking workshop (Lynett et al. 2017; NTHMP 2012). Please refer to Titov and Gonzalez (1997) for further information about MOST as well as general model validation.

MOST uses a series of nested grids to propagate the tsunami from the tsunami source to the small craft marinas. The coarsest grid, at 4-arc min resolution, covers the whole Pacific Ocean basin. Three additional grids of increasingly finer resolution help refine the numerical results as the wave propagates from the source to the marina. The innermost grid (known as the nearshore inundation grid) has a 10 m resolution, taking boundary input from the previous MOST nested layers. Each grid uses bathymetric and topographic data published the by National Oceanic and Atmospheric Administration's National Geophysical Data Center, specifically developed for tsunami forecasting and modeling efforts by Grothe et al. (2012) and Lynett et al. (2014).

Hydrodynamic model predictions of tsunami surface elevation are commonly compared with tide gauge data. Current speed comparisons are less common, principally due to the lack of data. Therefore, the MOST small craft marina modeling for California was validated against the high-order Boussinesq-type model

Cornell University Long and Intermediate Wave Modeling Package (COULWAVE) (Lynett et al. 2014). A comparison of MOST and COULWAVE results suggest that, while not as accurate as the higher-order COULWAVE model, the MOST tsunami model satisfactorily reproduces measured tsunami-induced current speeds and is conservative in its values (Lynett et al. 2014). MOST's conservative results and fractional run time (compared with COULWAVE) means MOST is an ideal tool for understanding tsunami-generated hydrodynamic hazards and risk within ports and harbors.

Marina Condition Assessment

Once the suite of tsunami events is modeled, the demand/capacity framework can be applied to a harbor. To apply the methodology, deterministic and probabilistic inputs are needed for the Monte Carlo modeling. Deterministic quantities are those that are known or are not expected to vary within a scenario. Deterministic quantities for floating docks include finger length, finger width, number of slips, number of piles, and number of cleats. These quantities were estimated from historical high-resolution orthoimagery data from USGS.

In contrast to deterministic inputs, probabilistic inputs are those quantities that might not be exactly known but can be defined by a probability density function to account for the associated uncertainty. These quantities could include current speed, current direction, water depth, sea water density, vessel length, vessel beam, and vessel draft. Each input variable was randomized, assuming a rectangular probability density function (e.g., equal probability of any value within range), bounded by defined minima and maxima and can be isolated from the modeling results.

For each slip, cleat and pile guide capacity were estimated from the site visit and tables outlined in section "Cleat and Pile Guide Capacities." It is common within a harbor to see a range of capacities as facilities managers update components and older sections of the harbor are replaced when damaged by tsunami events. In most of the surveys, aging hoop- or roller-type pile guides had been updated with HDPE pile guides if the infrastructure could support the redesign. While photographing every component within a harbor is not necessary, variability does point to the need to document general conditions within a harbor (e.g., roller pile guide versus HDPE pile guide) to accurately estimate risk at the parcel scale.

The demand/capacity framework was applied on a slip-by-slip basis. First, failure probability was estimated for each slip, and results were averaged over the entire dock finger. While the method can be applied without calibration and has been shown to give reasonable results, we included a calibration factor to allow us to calibrate the failure probabilities against known failure events. Without available calibration data, the recommended nominal calibration factor is 2.0, a value representative of the factor of safety applied during engineering design. The value is recommended for harbors inside and outside of California.

Damage reports from the harbors that sustained damage in the 2010 Chile tsunami and 2011 Tōhoku tsunami summarized in Wilson et al. (2013) were typically used for calibration by varying the calibration factor from 1.0 to 3.0. Incremental increases in the calibration factor produced calibration results that corresponded with a known tsunami scenario. The results were used to understand where the calibration shifts the results from one threshold to the next as a function of calibration factor. The calibration factor that reproduced the damage during the tsunami event was applied to the model for the remaining scenarios. The calibration factor for cleats and pile guides in California ranged from 1.8 to 2.2 depending on the harbor.

Results

Results for each harbor are presented as risk tables with low risk representing probability of failure $\leq$10%, medium risk representing probability of failure between 10% and 99% and high risk representing probability of failure $\geq$99%. While these limits may seem somewhat arbitrary, they were empirically derived based upon observed damage ratings. The ratings are outlined by Mesiti-Miller Engineering Inc. (2011) for recorded damage in Santa Cruz Harbor during the 2011 Tōhoku tsunami (Keen et al. 2017).

This basic approach has been applied to two dozen small craft marinas in California spanning from Oceanside Harbor in Southern California to Crescent City Harbor in Northern California. While we will focus here on one small craft marina in Northern California, Noyo River Harbor, our methodology should be valid for harbors along the US West Coast where smaller amplitude, long-period tele-tsunamis have the potential to impact on vessel and harbor operations. For nearfield tsunamis, Suppasri et al. (2014) and Muhari et al. (2015) have published a methodology to quantify vessel loss function based upon vessel data from the 2011 Tōhoku tsunami that would be more appropriate. Our approach presented here for tele-tsunamis and the one presented by Suppasri et al. (2014) and Muhari et al. (2015) were informed by correlations between numerically modeled tsunami characteristics and vessel damage. The inclusion of a calibration factor in our methodology will help generalize the approach to harbors outside of California.

Case Study: Noyo Harbor

Noyo Harbor District is a small port located along the Northern California Coast (see Fig. 1). The harbor is built near the mouth of the Noyo River in the town of Noyo, just south of Fort Bragg, California. Noyo Harbor consists of two basins. Noyo Basin is the largest of the two and harbors mostly commercial vessels. A map of Noyo Basin is shown in Fig. 7. Dolphin Basin, upriver from Noyo Basin, is the smaller of the two and harbors mostly recreational vessels; Dolphin Basin was not included in the survey. During the 2011 Japan tsunami, a series of waves caused significant damage to floating docks within Noyo Basin (Wilson et al. 2013). The ends of Docks B and C were torn from the pile guides. Since that event, the destroyed section of Dock B has been replaced, the end of Dock C has not.

Marina Condition Assessment and Risk-Model Calibration

A survey of Noyo Basin was conducted on March 10th, 2016. With 256 slips, we were able to photograph every slip and pile guide in the harbor. Representative cleats and pile guides from the survey are shown in Figs. 8 and 9, respectively. Frequent precipitation in Noyo River has caused the cleats and pile guides to corrode at a rate faster than average. With limited funds available to the facilities manager, the harbor is unable to keep up with the corrosion, which leaves it vulnerable to tsunami events.

The corrosion of the cleats and pile guides results in a severe reduction of the original capacities. Cleats were measured to be 250 mm (10-in.) during the field survey. M16 (1/2-in.) bolts are commonly associated with a 250-mm cleat (Sea-Dog Corporation 2018). The tension capacity of an M16 bolt (Grade 8.8) is 70.3 kN (British Standards 2005), which places the total new capacity of the cleat at 140.3 kN. An assessment of the cleat conditions based upon Table 1 and Fig. 8 places the cleat in the SD

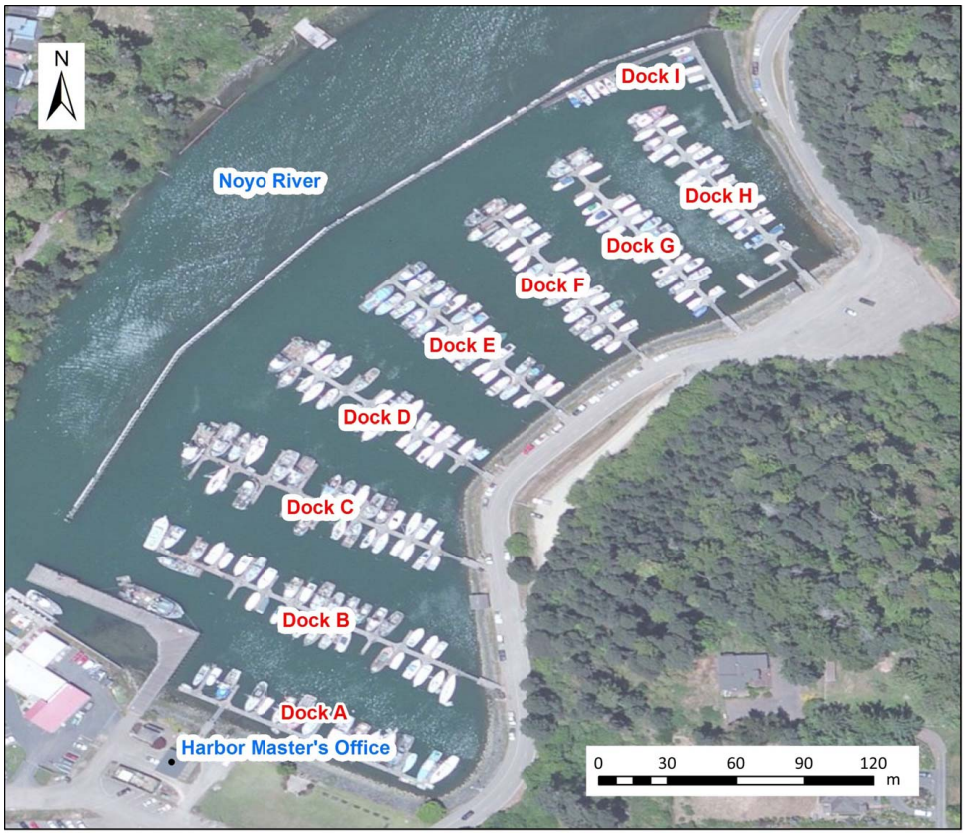

Fig. 7. Location of floating docks in Noyo Basin. (Aerial imagery courtesy of USGS.)

Fig. 8. Representative cleats from Noyo Basin. (Images by Adam S. Keen.)

class (Damage Class 5) range with corrosion exceeding 75% of the cleat. The cleat capacity range should therefore be between 0 and 35.1 kN (see Fig. 2).

The hoop-type pile guides were observed to be in a similar state with major corrosion, with fractional or missing section loss common across most of the hoop-type pile guides. The pile guides' proximity and exposure to the water further accelerates the aging process. Four M16 (1/2-in.) bolts are commonly associated with pile guides in Noyo River. The tension capacity of an M16 bolt (Grade 8.8) places the total capacity of the pile guide at 280.6 kN. An assessment of the pile guide conditions based upon Table 2 and Fig. 9 places the pile guide in the SD class (Damage Class 5) range with section loss present in many of the pile guide hoops. The pile guide capacity range should therefore be between 0 and 70.2 kN (see Fig. 2).

The cleat and pile guide damage of Noyo River Harbor was used to calibrate the structural capacities within the risk model to more accurately reflect conditions within the harbor. During the harbor visit on March 10th, we were able to ask the Noyo River harbormaster about the maintenance and damage history of the floating dock infrastructure. The harbormaster verified that the ends of Docks B and C failed during the 2011 tsunami event. Using this information, we calibrated the risk model via the cleat and pile guild capacity calibration factor, γ, by varying the calibration factor and running the various iterations representative of the 2011 tsunami event in Noyo River. The calibration is considered convergent

when the γ reproduces the reported damage (in this case high damage potential for Docks B and C). The calibration factor was then applied to the remaining tsunami events and scenarios. Calibrating against damage in Noyo River during the 2011 Japan event showed good agreement with observed capacities with the capacity scale factor equal to 2.1 for cleats and pile guides.

Since the damage that occurred to Noyo River in 2011, no significant upgrades to infrastructure have been undertaken, and only a small segment of the damaged floating docks has been replaced. We were therefore able to move forward with applying these damage classes and capacity scale factors to the suite of historic and probable tsunami event scenarios. If updates to the harbor had been performed since the 2011 tsunami, damage classes within the risk model could have changed (e.g., from Damage Class 5) to reflect the upgraded conditions and increased capacity (e.g., to Damage Class 1 or 2).

MOST was used to evaluate several historic and probable scenarios for Noyo River Harbor. The following events and scenarios were analyzed as part of this: the 2010 Magnitude 8.8 Chile event (historical), the Magnitude 9.0 Cascadia scenario, the 2011 Magnitude 9.0 Japan event (historical), the Magnitude 9.4 Chile North scenario, and the Magnitude 9.2 Eastern Aleutian-Alaska scenario.

Fig. 9. Representative pile guides from Noyo Basin. (Images by Adam S. Keen.).

Maximum current speed modeling results for the five scenarios are shown in Fig. 10. The two historical events were selected for Noyo River because of the amount of damage the tsunamis caused within the harbor, and documentation was available to validate the damage. The probable scenarios were selected because of their potential impacts on the harbor. The Magnitude 9.2 Eastern Aleutian-Alaska scenario would produce the strongest current velocities in Noyo River of any of the modeled events.

Results and Discussion

The results of the cleat analysis (Fig. 11) indicated that Noyo Basin is most vulnerable to the Magnitude 9.2 Eastern Aleutian-Alaska scenario. The modeling indicated that Docks B, C, and D have a high level of vulnerability while Docks A, E, F, G, and H have a moderate level of vulnerability. The MOST results suggested that the current speeds increase near the harbor entrance (near Docks B, C, and D), generating heterogeneous damage potential. After the Aleutian-Alaska scenario, the results indicated that the next event Noyo Basin would be most vulnerable to was the Magnitude 9.0 Cascadia scenario. In terms of all scenarios, Dock B would be most vulnerable to the modeled tsunami events, with two of the six events indicating high vulnerability and four indicating moderate vulnerability. The next most vulnerable would be Docks C and D.

Like the cleat analysis, the results of the pile guide analysis (Fig. 12) indicated that Noyo Basin is most vulnerable to the Magnitude 9.2 Eastern Aleutian-Alaska scenario. The modeling indicated that Docks B, C, D, and E have a high level of vulnerability, while Docks A, F, G, and H have a moderate level of vulnerability. After the Aleutian-Alaska scenario, the results indicated that the next event Noyo Basin would be vulnerable to was the Magnitude 9.0 Cascadia scenario. In terms of all scenarios, Dock B would be most vulnerable to the modeled tsunami events, with two of the six events indicating high vulnerability and four indicating moderate vulnerability. The next most vulnerable would be Docks C, D, and E.

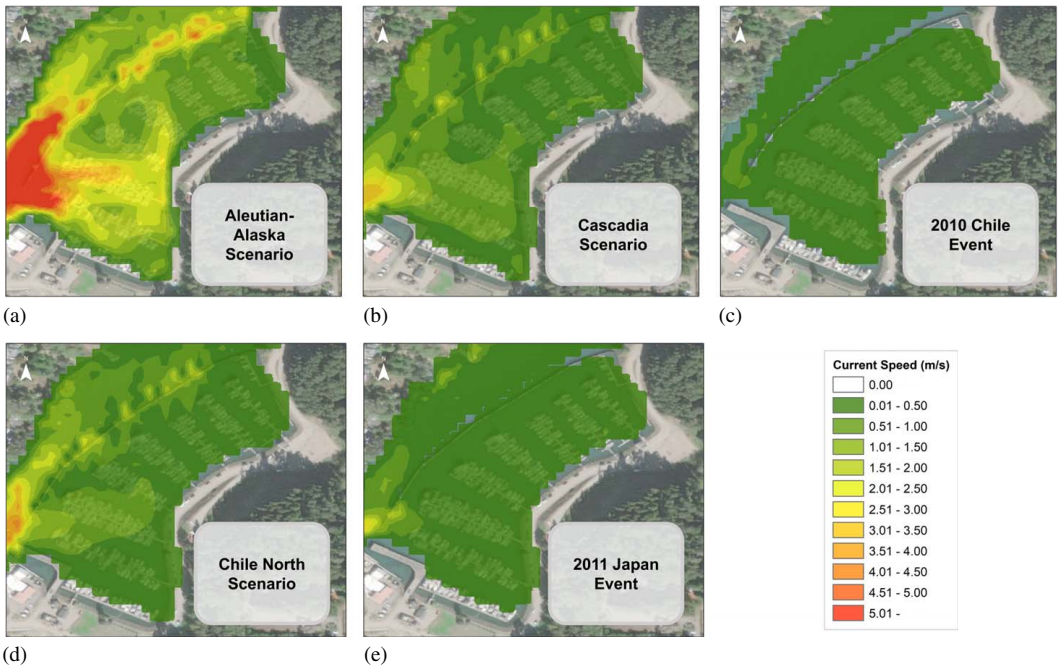

Fig. 10. Numerical modeling results of maximum current speed (by tsunami scenario/event) within Noyo Basin: (a) Aleutian-Alaska scenario; (b) Cascadia scenario; (c) 2010 Chile event; (d) Chile North scenario; and 2011 Japan event. (Aerial imagery courtesy of USGS.)

Tsunami Event/Scenario	Dock								
	A	B	C	D	E	F	G	H	I
Magnitude 9.2 Eastern Aleutian-Alaska Scenario	Moderate	High	High	High	High	Moderate	Moderate	Moderate	Low
Magnitude 9.0 Cascadia Scenario	Moderate	High	Moderate	Moderate	Moderate	Moderate	Moderate	Moderate	Low
2010 Magnitude 8.8 Chile Event (Historical)	Low	Moderate	Low	Low	Low	Low	Low	Low	Low
Magnitude 9.4 Chile North Scenario	Moderate	Moderate	Moderate	Moderate	Moderate	Moderate	Moderate	Moderate	Low
2011 Magnitude 9.0 Japan Event (Historical)	Low	Moderate	Moderate	Moderate	Moderate	Low	Low	Low	Low

Fig. 11. Cleat probability of failure results for Noyo River Basin. Low risk representing probability of failure <10%, medium risk representing probability of failure between 10% and 99%, and high risk representing probability of failure >99%.

Tsunami Event/Scenario	Dock								
	A	B	C	D	E	F	G	H	I
Magnitude 9.2 Eastern Aleutian-Alaska Scenario	Moderate	High	High	High	High	Moderate	Moderate	Moderate	Low
Magnitude 9.0 Cascadia Scenario	Moderate	High	Moderate	Moderate	Moderate	Moderate	Moderate	Moderate	Low
2010 Magnitude 8.8 Chile Event (Historical)	Low	Moderate	Low	Low	Low	Low	Low	Low	Low
Magnitude 9.4 Chile North Scenario	Moderate	Moderate	Moderate	Moderate	Moderate	Moderate	Moderate	Moderate	Low
2011 Magnitude 9.0 Japan Event (Historical)	Low	Moderate	Moderate	Moderate	Moderate	Moderate	Low	Low	Low

Fig. 12. Pile guide probability of failure results for Noyo River Basin. Low risk representing probability of failure <10%, medium risk representing probability of failure between 10% and 99%, and high risk representing probability of failure >99%.

The strength of our probabilistic risk methodology is the method's ability to characterize not only the tsunami hazard but also the infrastructure vulnerability. Previous approaches by Lynett et al. (2014) and Keen et al. (2017), focus primarily on capturing the tsunami hazard as a bulk property of tsunami damage. Lynett et al. (2014) for instance provides a rudimentary damage threshold based upon the maximum current speeds. For current speeds less than 1.5 m/s, no damage is expected; for current speeds greater than 4.5 m/s, extreme damage (structural failure) is possible. Our results suggested significant damage in Noyo River occurred with a current speed less than 4.5 m/s during the 2011 tsunami (see Fig. 10). This result, along with the cleat and pile guide results from the risk model, suggested that the underlying condition (infrastructure vulnerability) of the cleats and floating docks is ultimately responsible for future damage potential, summarized in Figs. 11 and 12.

Conclusions

The aim of this paper is to present a risk framework that can be used by harbor maintenance and decision makers to assess future tsunami risks to small craft harbors in California. The methodology was based on the demand-to-capacity ratio of a floating dock system with physics-based probabilistic inputs used to characterize uncertainty in the demand. Empirically derived probabilistic inputs were used to characterize uncertainty in the capacity. An extensive field campaign that included a survey of damage states within 12 California harbors was carried out over the course of 2 years. The campaign included failure modes and damage states (representative of the infrastructure aging process) that allowed the authors to empirically derive these capacity estimates.

When applied to a small craft marina, Noyo River Harbor, the method was able to characterize the historic observed damage in the harbor from the 2011 tsunami event with little calibration. Although the tsunami-generated currents in Noyo River were small relative to many other marinas in California, the method presented here accurately characterized the vulnerability of the harbor and the resultant risk. The results illustrated the balance between event hazard and infrastructure vulnerability that ultimately contribute to Noyo River's tsunami risk.

Coupling the approach with future tsunami scenarios provides risk managers with a reliable method to characterize vulnerabilities within the harbor. With limited resources available across all levels of government, optimizing the return on investment is the primary consideration for decision makers. The method presented in this paper provides a direct quantitative estimate that decision makers can use to quantify their return on investment (cost-benefit) and relative risk reduction for any mitigation project.

Data Availability Statement

Some or all data, models, or code that support the findings of this study are available from the corresponding author upon reasonable request. Available data includes MOST hydrodynamic modeling results (Fig. 10) for Noyo River Harbor as well as the statistical modeling for cleats (Fig. 11) and pile guides (Fig. 12).

References

Barberopoulou, A., M. R. Legg, B. Uslu, and C. E. Synolakis. 2011. "Reassessing the tsunami risk in major ports and harbors of California I: San diego." *Nat. Hazards* 58 (1): 479–496. https://doi.org/10.1007/s11069-010-9681-8.

British Standards. 2005. "Eurocode 3. Design of steel structures. Material toughness and through-thickness properties (BS EN 1993-1-10:2005)." London, UK: BSI.

Borrero, J. C., and D. G. Goring. 2015. "South American tsunamis in Lyttelton Harbor, New Zealand." *Pure Appl. Geophys.* 172 (3–4): 757–772. https://doi.org/10.1007/s00024-014-1026-1.

Borrero, J. C., D. G. Goring, S. Dougal Greer, and W. L. Power. 2015a. "Far-field tsunami hazard in New Zealand Ports." *Pure Appl. Geophys.* 172 (3–4): 731–756. https://doi.org/10.1007/s00024-014-0987-4.

Borrero, J. C., P. J. Lynett, and N. Kalligeris. 2015b. "Tsunami currents in ports." *Philos. Trans. R. Soc. London, Ser. A* 373 (2053): 20140372. https://doi.org/10.1098/rsta.2014.0372.

Dengler, L., B. Uslu, A. Barberopoulou, S. C. Yim, and A. Kelly. 2009. "Tsunami damage in crescent city, California from the November 15, 2006 Kuril event." *Pure Appl. Geophys.* 166 (1–2): 37–53. https://doi.org/10.1007/s00024-008-0429-2.

Dewan, A. 2013. *Floods in a megacity: Geospatial techniques in assessing hazards, risk and vulnerability*. 1st ed. Springer Geography. Dordrecht, Netherlands: Springer.

Grothe, P. G., L. A. Taylor, B. W. Eakins, K. S. Carignan, D. Z. Friday, and M. Love. 2012. Digital elevation models of monterey. California: Procedures, Data Sources and Analysis. National Geophysical Data Center.

Keen, A. S., P. J. Lynett, M. L. Eskijian, A. Aykut, and W. Rick. 2017. "Monte carlo–based approach to estimating fragility curves of floating docks for small craft marinas." *J. Waterw. Port Coastal Ocean Eng.* 143 (4): 04017004. https://doi.org/10.1061/(ASCE)WW.1943-5460.0000385.

Lynett, P. J., et al. 2017. "Inter-Model analysis of tsunami-induced coastal currents." *Ocean Modell.* 114: 14–32. https://doi.org/10.1016/j.ocemod.2017.04.003.

Lynett, P. J., J. Borrero, S. Son, R. Wilson, and K. Miller. 2014. "Assessment of the tsunami-induced current hazard." *Geophys. Res. Lett.* 41 (6): 2048–2055. https://doi.org/10.1002/2013GL058680.

Lynett, P. J., J. C. Borrero, R. Weiss, S. Son, D. Greer, and W. Renteria. 2012. "Observations and modeling of tsunami-induced currents in ports and harbors." *Earth Planet. Sci. Lett.* 327–328: 68–74. https://doi.org/10.1016/j.epsl.2012.02.002.

Mesiti-Miller Engineering Inc. (2011). Tsunami damage evaluation of all fixed and floating facilities at the Santa Cruz small craft harbor. Prepared for Santa Cruz Port District.

Muhari, A., I. Charvet, F. Tsuyoshi, A. Suppasri, and F. Imamura. 2015. "Assessment of tsunami hazards in ports and their impact on marine vessels derived from tsunami models and the observed damage data." *Nat. Hazards* 78 (2): 1309–1328. https://doi.org/10.1007/s11069-015-1772-0.

NTHMP (National Tsunami Hazard Mitigation Program). 2012. *Proceedings and results of the 2011 NTHMP model benchmarking workshop*. Boulder, CO: U.S. Dept. of Commerce/NOAA/NTHMP.

Okada, Y. 1985. "Surface deformation due to shear and tensile faults in a half-space." *Bull. Seismol. Soc. Am.* 75 (4): 1135–1154.

Rabbat, B. G., and H. G. Russell. 1985. "Friction coefficient of steel on concrete or grout." *J. Struct. Eng.* 111 (3): 505–515. https://doi.org/10.1061/(ASCE)0733-9445(1985)111:3(505).

Ross, S. L. et al. 2013. *SAFRR (science application for risk reduction) tsunami scenario–executive summary and introduction: Chapter A in the SAFRR (science application for risk reduction) tsunami scenario*. Rep. No. 2013-1170A. Open-File Report. Reston, VA: USGS Publications Warehouse.

Sea-Dog Corporation. 2018. "Dock cleat - Hex head: Hot dipped galvinized iron." *Sea-dog corporation*. http://www.sea-dog.com/groups/7-dock-cleat-hex-head.

Suppasri, A., A. Muhari, T. Futami, F. Imamura, and N. Shuto. 2014. "Loss functions for small marine vessels based on survey data and numerical simulation of the 2011 great east Japan tsunami." *J. Waterw. Port Coastal Ocean Eng.* 140 (5): 04014018. https://doi.org/10.1061/(ASCE)WW.1943-5460.0000244.

Titov, V. V., and F. Gonzalez. 1997. Implementation and testing of the method of splitting tsunami (MOST) model. US Department of Commerce, National Oceanic and Atmospheric Administration, Environmental Research Laboratories, Pacific Marine Environmental Laboratory.

Titov, V., and C. Synolakis. 1998. "Numerical modeling of tidal wave runup." *J. Waterw. Port. Coast. Ocean Eng.* 124 (4): 157–171. https://doi.org/10.1061/(ASCE)0733-950X(1998)124:4(157).

USACE, NAVFAC, and AFCESA (U.S. Army Corps of Engineers, Naval Facilities Engineering Command, and Air Force Civil Engineer Support Agency). 2005. *Design: Moorings. unified facilities criteria*. Scotts Valley, CA: CreateSpace.

Waterfront Inspection Task Committee. 2015. *Waterfront facilities inspection and assessment.* Vol. 130 of *manuals of practice*. Reston, VA: ASCE.

Wilson, R., et al. 2013. "Observations and impacts from the 2010 Chilean and 2011 Japanese tsunamis in california (USA)." *Pure Appl. Geophys.* 170 (6–8): 1127–1147. https://doi.org/10.1007/s00024-012-0527-z.

Zhang, H. 2016. "Surface characterization techniques for polyurethane biomaterials." Chap. 2 in *Advances in polyurethane biomaterials*, edited by S. L. Cooper, and J. Guan, 23–73. Cambridge, UK: Woodhead Publishing.